Article:
Srinivas, Krishnan, Gilio, Amelia, Sharma, Mahima et al. (2025) Structures of 'Tyrosine-IRED' IR91 from Kribbella flavida in Complex with a Reductive Amination Substrate and Product. Chembiochem. e202500450. ISSN: 1439-7633

https://doi.org/10.1002/cbic.202500450

Structures of 'Tyrosine-IRED' IR91 from *Kribbella flavida* in Complex with a Reductive Amination Substrate and Product

Krishnan Srinivas,[a] Amelia K. Gilio,[a] Mahima Sharma,[a] Lawrence Green,[a] Alexander Ascham,[a] Jack Domenech,[a] Balázs Pogrányi,[a] Jiacheng Li,[a] Scott P. France,[b] Russell D. Lewis,[c] William P. Unsworth,[a] and Gideon Grogan*[a]

Abstract: Imine reductases with an (*S*)-preference for the reduction of the model substrate 2-methyl pyrroline typically contain tyrosine in the active site (Y-IREDs) instead of the aspartate present within (*R*)-selective enzymes (D-IREDs). As with D-IREDs, a subset of Y-IREDs is capable of enabling reductive amination reactions between some ketone and amine partners to give optical active amines with high optical purity. However, structures of Y-IREDs in complex with the substrates and products of the reductive amination have not been forthcoming. Here we present structures of the Y-IRED IR91 from *Kribbella flavida* in complex with 5-methoxy-2-tetralone, a synthetic precursor to the anti-Parkinson's treatment rotigotine, and also its reductive amination product with methylamine, 5-methoxy-(*S*)-2-(*N*-methylamino)-tetralin. The structures, in combination with mutation and kinetic studies, support a role for tryptophan residue W258 in the activity of the enzyme, possibly in binding of the ketone prior to reaction with methylamine.

Introduction

Imine Reductases (IREDs) are now established as important catalysts for the preparation of chiral amines,[1,2] either through the NADPH-dependent asymmetric reduction of cyclic imines,[3-6] or as Reductive Aminases (RedAms),[7-13] which catalyze both imine formation and imine reduction when presented with equimolar quantities of ketone and amine partners. Studies of multiple IREDs have revealed subgroups of the enzymes that are capable of either the (*R*)- or (*S*)-selective reduction of the model imine substrate 2-methylpyrroline **1** to 2-methylpyrrolidine **2** (**Scheme 1A**).[3] Structural studies of these two sub-groups of enzymes have revealed that, in most cases, the first have an aspartate (Asp, D) residue that projects from the top of the active site towards the nicotinamide ring of the NADPH cofactor (D-IREDs),[14] and that the latter have a tyrosine residue (Tyr, Y) in the same position (Y-IREDs).[15,16] The (*R*)- and (*S*) selectivity has been in some cases retained for reductive amination reactions. For example, in a previous study by Pfizer[17] it was shown that the D-IRED IR46 from *Streptomyces* CNS615 catalyzed the reductive amination of 2-tetralone **3** with methylamine **a** to give the (*R*)-amine product **3a** with >98% e.e., whereas the Y-IRED IR91 from *Kribbella flavida* catalyzed the transformation to give the (*S*)-product, also with >98% e.e. (**Scheme 1B**).

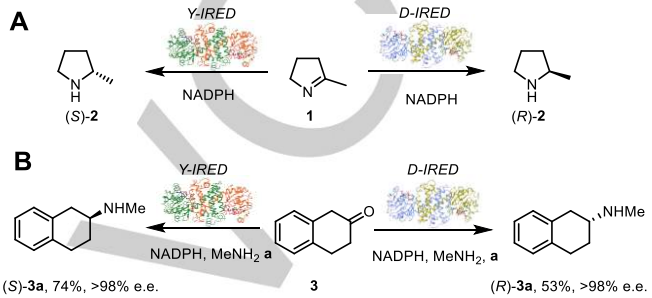

Scheme 1. **A**: Reduction of 2-methylpyrroline **1** by D- and Y-IREDs; **B**: Reduction of 2-tetralone **3** by enantiocomplementary D- and Y-IREDs.[18]

While the roles of the aspartate and tyrosine residues in imine reduction reactions have not been conclusively explained, mutation of the former to alanine,[14] or of the latter to alanine or phenylalanine,[16,18] gave variants of low or no measurable activity. With respect to reductive amination reactions, in the case of D-IREDs such as *Asp*RedAm and *At*RedAm, a combination of structural studies and mutation have suggested that, in the case of smaller, hydrophobic amines, the residue may plausibly act as a base for the activation by deprotonation of the amine to create a more potent nucleophile for the imine formation reaction.[19] This hypothesis was based on structures of *At*RedAm in complex with ketone, amine and also the redox-inactive cofactor $NADPH_4$, in combination with kinetic studies of the Asp to Ala mutant.[19] In the case of Y-IREDs however, there were, until recently, no structures in complex with ketone or amine ligands at all, meaning that any relationship between the active site residues and ternary ligands had not been established. Recently, Zheng and co-workers have presented the first structures of Y-IREDs in complex with $NADP^+$ and cyclic imine substrates.[20] In some of these structures (PDB ID 7Y8N, 7Y8O), the amine nitrogen of the imine is sometimes well-aligned to interact with the Tyr phenolic hydroxyl, but in others (PDB ID 6JIT, 7Y8L), it is somewhat distant and therefore the authors suggest that this Tyr is less involved in catalysis in some instances.[20]

In this study, we sought to obtain more information on the relationship between active site residues and substrates/products in *reductive amination* reactions catalyzed by Y-IREDs, as no previous structural information was available for this sub-group working in this mode. We chose as our model the enzyme 'IR91' from *Kribbella flavida*, the activity of which had been studied previously.[17] The results reveal the structural relationship between substrate and product ligands and the active site and the possible involvement of a tryptophan residue W258 in the activity of the enzyme.

Results and Discussion

IR91 (the amino acid sequence is given in **Figure S1**) was identified as an enzyme of interest as it had been shown to enable the reductive amination of some bulky ketone substrates, and also with some bulkier amines, in previous work.[17] The gene encoding IR91 (**Figure S2)** was synthesised, equipped with an N-terminal hexahistidine tag

[a] Mr K. Srinivas, Dr A.K. Gilio, Dr M. Sharma, Mr L. Green, Mr A. Ascham, Mr J. Domenech, Dr B. Pogrányi, Dr J. Li, Dr W.P. Unsworth, Prof. Dr. G. Grogan
Department of Chemistry
University of York
Heslington York YO10 5DD UK
gideon.grogan@york.ac.uk
[b] Dr Scott P. France
Process Research and Development
Merck & Co., Inc., Rahway, NJ 07065, USA
[c] Dr R. D. Lewis
Pfizer Worldwide Research and Development
445 Eastern Point Road Groton Connecticut 06340 USA

Supporting information for this article is given via a link at the end of the document

and provided in a pET-28a vector. The gene was expressed in *E. coli* and purified using nickel affinity (**Figure S3**) and size exclusion chromatography (SEC) (**Figure S4**). The activity of the purified enzyme was confirmed with biotransformation studies using cyclohexanone **4**, along with methylamine **a** as the amine partner and a cofactor recycling system made up of $NADP^+$, glucose-6-phosphate dehydrogenase (G6PDH) and glucose-6-phosphate (G6P), as previously described (**Scheme 2**).[17] Smooth conversion of starting materials to product was observed, leading to quantitative conversion over a 24 h period (**Figure S5**).

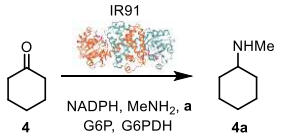

Scheme 2. **A**: Reductive amination of cyclohexanone **4** with methylamine **a** by IR91.[17]

The activity of IR91 was also evaluated using kinetic measurements with cyclohexanone **4** and methylamine **a** as substrates (**Figures S6A** and **S6B**). IR91 displayed a K_m of 29 mM and a k_{cat} of 0.05 s^{-1} for cyclohexanone, measured at a constant concentration of 96 mM methylamine, and a K_m of 184 mM for methylamine at an invariant concentration of 10 mM cyclohexanone (**Table 1**). The figures for cyclohexanone indicate that IR91 is a poorer catalyst overall for this transformation than other IREDs, including *Asp*RedAm (K_m (**4**) 1.90 mM; k_{cat} 1.47 s^{-1})[9] and *At*RedAm (K_m (**4**) 2.10 mM; k_{cat} 0.11 s^{-1}).[19]

Purified IR91 was subjected to crystallisation trials with different ligand mixtures in an attempt to yield binary and ternary complexes. These included $NADP^+$, but also 2-tetralone **3**, 5-methoxy-2-tetralone **5** and their racemic methylamine products **3a** and **5a** (**Scheme 3**), which were synthesised using the published procedures for reductive amination of tetralones (**SI Section 7**). Ketone **5** is of interest as a reductive amination substrate, as a RedAm-catalyzed *n*-propyl amination of **5** has been incorporated into the asymmetric synthesis of the dopamine agonist (*S*)-rotigotine **5c** by Turner and co-workers (**Scheme 3**).[21]

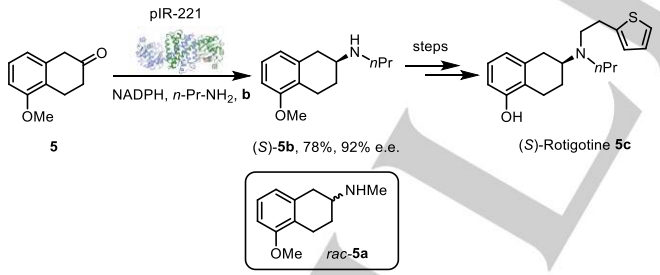

Scheme 3. Biotransformation of 5-methoxy tetralones by (*S*)-selective IRED pIR-221.[21]

In the first instance, a structure of IR91 in complex with only the cofactor $NADP^+$ (IR91-$NADP^+$, PDB ID **9R76**) was obtained (Data collection and refinement statistics can be found in **SI Section 8 Table S1**). This structure, which was refined to 1.49 Å, contained two molecules in the asymmetric unit (asu) representing one dimer. The structure of IR91 displayed the canonical IRED fold, with two monomers associating to form a dimer with the active site at the monomer-monomer interface (**Figure 1**). The monomer structure was found to be most similar to the Y-IREDs PDB ID 6JIT from *Stackebrandtia nassauensis* DSM 44728 (60% sequence identity; rmsd 1.4 Å over 290 Cα atoms) and 4OQY from *Streptomyces* sp. GF3546 (46%, 1.8 Å over 268 Cαs).[15] as determined by the DALI server.[22] An amino acid sequence alignment of IR91 with these enzymes and also the Y-IRED from *S. clavuligerus* studied by Zheng (PDB ID 7Y8N *etc.*)[20] is given in **Figure S9**.

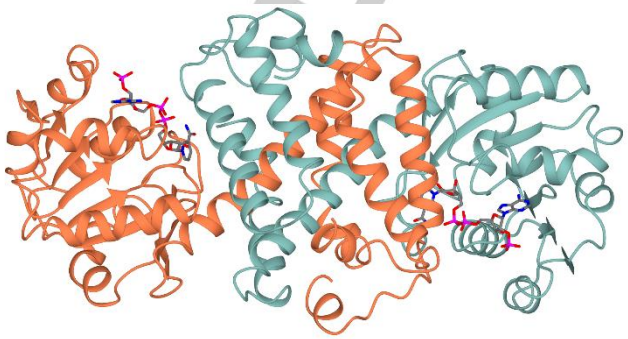

Figure 1. Structure of IR91 dimer (IR91-$NADP^+$) in ribbon format with subunits shown in green and coral and $NADP^+$ (carbon atoms in grey) bound at the active sites

Clear electron density in the omit maps was observed at both of the active sites of IR91 and this was successfully modelled in both as the cofactor $NADP^+$. The second and third structures, which were derived from data from crystals that had been co-crystallised with **5** and *rac*-**5a** respectively, also had one dimer in the asu and were refined to resolutions of 1.80 Å (IR91-$NADP^+$-**5**, PDB ID **9R79**) and 1.91 Å (IR91-$NADP^+$-**5a**, **9R7A**). Each was obtained in complex with $NADP^+$ but residual omit density in the active site adjacent to the nicotinamide ring also permitted modelling and refinement of **5** (**Figure 2A**) and (*S*)-**5a** (**Figure 2B**) respectively. Substrate complex IR91-$NADP^+$-**5** can be used to describe the features of the active site with respect to other Y-IREDs such as PDB ID 6JIT (**Figure S10A**) and 7Y8N. In addition to the pendant tyrosine (A)Y172 (*Y171* in 6JIT) that classifies the enzyme as a Y-IRED, the hydrophobic residues in the binding cleft are well conserved between the two, including (A)L176 (*L175*) and (A)L180 (*L179*) on the wall of the active site opposite the nicotinamide ring of the cofactor, although another residue on this wall – (A)F179 (*L178*) - is larger in IR91. At the floor of the active site as illustrated in **Figure 2A** is (B)W285 (*W287*) and at the front, (B)M243 and (B)M244 also from the partner monomer. At the rear of the active site, the hydrophobic pocket is completed by M217 (*M216*) and (A)P125 (*P124*). Ligand **5** is positioned with the aromatic ring of the tetralone ring stacked against the nicotinamide ring on one face and the side chain of (A)F179 on the other, with the aryl methoxy group pointed towards Y172 (**Figure 2A**). The side-chain of Y172, which has been shown to be essential for activity in related Y-IREDs[16,18] is far from the ketone group in this complex. Instead, the carbonyl group of the ketone interacts with the heterocyclic NH group of the side chain of W285, at a distance of 3.6 Å. The ketone is clearly not well positioned for reduction as the electrophilic carbon of the C=O group is 6.3 Å from the C4 atom of the $NADP^+$ that accepts and delivers hydride. However, these and other IREDs usually display negligible activity for ketone reduction to alcohol products, so an unfavourable pose for reduction might be expected for this ligand.

The IR91-$NADP^+$-**5a** complex (**Figure 2B**), obtained through co-crystallisation of IR91 with *racemic* **5a**, suggests preferential binding of the (*S*)-configured reductive amination product, which is the

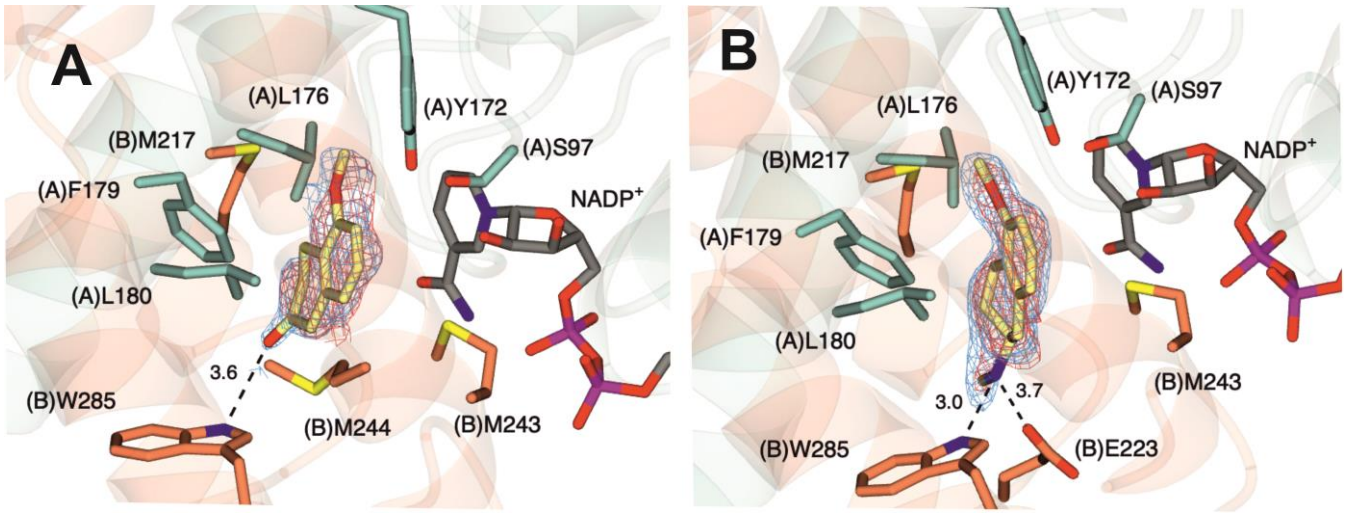

Figure 2: Active site of IR91 in complex with **A**: NADP$^+$ and **5**; **B**: NADP$^+$ and **5a**. In both frames **A** and **B**, the carbon atoms of backbone and side-chains of subunits (A) and (B) of the dimer are coloured in green and coral respectively. Electron density in blue and red corresponds to the $2F_o$-F_c and F_o-F_c omit maps at levels of 0.9 and 2.5 σ respectively and is that obtained prior to refinement of the ligand atoms. Selected interactions are shown by black dashed lines, with distances given in Ångstroms. In frame **A**, the side chain of E223 is omitted as it could not be modelled. In frame **B**, the side-chain of (B)M244 has been omitted so as not to obscure ligand **5a**.

enantiomer that would result from hydride delivery to the *re*-face of a prochiral methylamine intermediate. The (*S*)-configuration is the same as that observed experimentally for the methylamination of **3** by IR91 previously reported.[17] In order to confirm the stereoselectivity experimentally, IR91 was challenged with both **3** and **5** with methylamine as the reductive amination partner. The conversions for **3** and **5** were 88% and 33% as determined by NMR and the *ee*s of **3a** and **5a** were 97% and 99%. The major enantiomer of product **5a** eluted as the second of the peaks on chiral HPLC (**Figure S11C** and **S11D**), as did the known (*S*)-enantiomer of **3a** (**Figure S11A** and **S11B**), so we extrapolate that the stereoselectivity for methylamination of **3** by IR91 is retained for the methylamination of **5** by the same enzyme.

The mode of binding of (*S*)-**5a** is very similar to that observed in ketone complex IR91-**5.** The aryl methoxy group again points towards the side-chain of Y172, which is distant from amine group. The amine nitrogen of **5a** is closer to the NH group of (B)W285, at a distance of approximately 3.0 Å. The amine nitrogen also interacts with the side chain of E223, which could not be modelled in the IR91-NADP$^+$-**5** complex, at a distance of 3.7 Å. As with the IR91-NADP$^+$-**5** complex, the C2 carbon atom of the amine (which would be the electrophilic atom of the intermediate imine to receive a hydride in the reduction process) is too distant (6.9 Å) from the C4 atom of the NADP$^+$ nicotinamide ring for this to be a pose congruent with the requirements for hydride exchange. This suggests relocation of the product following imine reduction by the enzyme, possibly as it leaves the active site. The interaction of both **5** and **5a** with W285 is interesting however, as in the Y-IRED PDB ID 4OQY, this residue is substituted by a phenylalanine (**Figure S9; Figure S10B**). 4OQY did not appear to perform in a classical RedAm mode in the reductive amination of substrates, requiring 12.5-fold amine equivalents to achieve only low conversion in the methylamination of 4-phenyl-2-butanone.[15]

The ligand interactions suggested a possible role in the reaction mechanism for coordination of the carbonyl group of the ketone by W285 and in amine activation by E223, roles suggested to be fulfilled by a tyrosine and an aspartate residue in D-IREDs such as *At*RedAm.[19] In such a hypothetical mechanism (**Scheme 4**)., following amination, the imine intermediate **6** would have to translate forwards in the active site (as shown in **Figure 2A**) from the position of the ketone in the IR91 complex with **5** for the electrophilic carbon of the C=N bond to be adjacent to C4 of NADP/H for reduction.

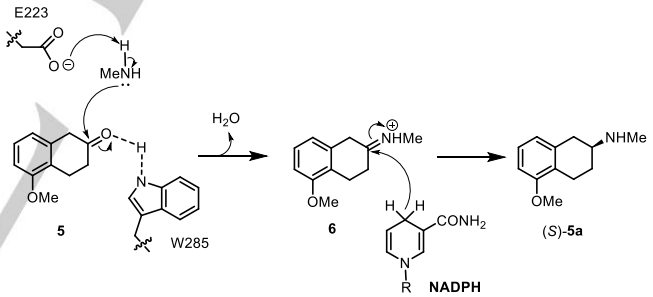

Scheme 4. Hypothetical roles of E223 and W258 in mechanism of reductive amination of 5-methoxy tetralone **5** by IR91, to be tested by mutation and analysis reported in **Table 1**.

Possible roles in catalysis for W285, E223 and Y172 were investigated through their mutation to alanine (**SI Section 11**) and kinetic analysis of the variants using cyclohexanone **4** and methylamine **a** as substrates (**Table 1**, **Figure S7, S8**). Mutation of W285 to alanine gave a mutant W285A of negligible activity, suggesting a previously unobserved role for an amino acid in the active site of a Y-IRED, which may be in the binding and activation of the carbonyl group prior to amination as suggested. By contrast, the E223A mutant retained wild-type like k_{cat} and K_m values within the margins of error, suggestive of no critical role in catalysis for this residue. A mode for amine activation in a reductive amination mechanism by IR91 remains cryptic therefore. In common with other studies on the mutation of the pendant tyrosine residue Y172,[18] no activity was detected using the NADPH oxidation assay nor NADPH-dependent biotransformations of **4** with **a** analysed by GC. Although the ligand complexes presented here do not support a direct role in catalysis for Y172, it is notable that the side chain phenol, along with the side chain of T247, bind a water molecule that is in close contact with the 2'-hydroxyl of the cofactor ribose, so an essential role in

Table 1: Kinetic constants for wt-IR91 and variants. n.m. = not measurable. Kinetic constants for **4** were measured using 0-90 mM **4** at a constant concentration of 96 mM **a**; Values for **a** were measured using 0-480 mM **a**t a constant concentration of 10 mM **4**.

Variant	K_m 4 (mM)	K_m a (mM)	k_{cat} (s^{-1})
WT	29 ± 6	184 ± 38	0.05 ± 5 x 10^{-3}
W285A	n.m.	n.m.	n.m.
E223A	27 ± 4	226 ± 57	0.05 ± 3 x 10^{-3}
Y172A	n.m.	n.m.	n.m.

cofactor binding by Y172 can not be ruled out.

Conclusion

Imine reductases and the reductive aminase subgroup have assumed an important role as catalysts for the selective and sustainable generation of chiral amine intermediates on an industrial scale. Structural information on these enzymes helps to characterise protein-ligand interactions, thus informing engineering studies that look to improve or alert their activity, In determining the structure of an (*S*)-selective Y-IRED in complex with both a substrate and reductive amination product, a platform is provided for mutational studies that will look to learn more about mechanism and engineer expanded and altered substrate specificity for bulkier ketones and amines.

Experimental Section

Gene Cloning and Expression

The amino acid sequence of IR91 is shown in **Figure S1**. The amino acid sequence was used to design a gene encoding IR91 that was codon-optimised for expression in *E. coli* (**Figure S2**). The gene was purchased inserted into a pET28a vector, which was used to transform *E. coli* BL21 (DE3) cells for expression. One colony from the transformation plates was inoculated into a 50 mL Falcon tube containing 10 mL LB media and 10 µL kanamycin (30 mg mL^{-1}). These overnight cultures were then left to grow overnight at 37ºC with shaking at 180 rpm. Each 10 mL culture of LB media containing grown cells was then inoculated into a 2.5 L shaker flask containing 1 L freshly autoclaved LB Media and 1 mL of kanamycin (30 mg mL^{-1}). This was left shaking for 1 h at 37ºC until the cultures reached an optical density, measured at 600 nm, of 0.6-0.8. To each flask was then added 1 mL of 1 M β-D-1-thiogalactopyranoside (IPTG) to induce expression of the IR91 gene. The flasks were then left overnight at 16ºC, with shaking at 180 rpm.

Enzyme Purification

One colony from the transformation plates was inoculated into a 50 mL Falcon tube containing 10 mL LB media and 10 µL kanamycin (30 mg mL^{-1}). These overnight cultures were then left to grow overnight at 37ºC with shaking at 180 rpm. Each 10 mL culture of LB media containing grown cells was then inoculated into a 2.5 L shaker flask containing 1 L freshly autoclaved LB Media and 1 mL of kanamycin (30 mg mL^{-1}). This was left shaking for 1 h at 37ºC until the cultures reached an optical density, measured at 600 nm, of 0.6-0.8. To each flask was then added 1 mL of 1 M β-D-1-thiogalactopyranoside (IPTG) to induce expression of the IR91 gene. The flasks were then left overnight at 16ºC, with shaking at 180 rpm. All cells were harvested by centrifugation and resuspended in 10 mL buffer per L of cell growth containing 50 mM Tris-HCl and 300 mM NaCl at pH 7.5. Cells were disrupted using ultrasonication, and the filtered supernatant applied to a His-trap FF Crude Column (Cytiva), which was eluted with a linear gradient of imidazole from 0-300 mM over 10 column volumes. Column fractions were analysed bySDS-PAGE (**Figure S3**) and those revealed to contain IR91 were pooled, concentrated, and loaded onto a HiLoad 16/600 Superdex 75 gel filtration column pre-equilibrated with buffer containing 50 mM Tris-HCl pH 7.5 and 300 mM NaCl. Fractions from the SEC column were analysed by 12 % acrylamide SDS PAGE (**Figure S4**) and those containing IR91 were pooled for use in enzyme assays and crystallizations.

Kinetics

Kinetic constants for IR91 and mutants W285A and E223A were determined by measuring the oxidation of NADPH in the presence of cyclohexanone **4** and methylamine **a** using a Cary UV spectrophotometry at a wavelength of 340 nm. To obtain kinetic constants for cyclohexanone, the reaction included 0-90 mM cyclohexanone and 96 mM methylamine from a buffered stock solution adjusted to pH 9, with 0.5 mM NADPH. Oxidations of NADPH were monitored for 2 min in each reaction. Non-linear regression based on Michaelis Menten kinetics was then used for further data processing to obtain kinetic constants, using Origin® software. The results for wild-type IR91 are shown in **Figure S6A**. A similar protocol was used to obtain kinetic constants for IR91 with methylamine. A typical reaction mixture consisted of 0 - 480 mM methylamine, 10 mM cyclohexanone and 0.5 mM NADPH. The results for wild-type IR91 are shown in **Figure S6B**. **Figures 7A/B** and **8A/B** show the plots obtained for the W285A and E223A mutants respectively.

Synthesis of Amine Standards[23]

To a flame dried round bottom flask containing a magnetic stirring bar was added the corresponding ketone **3** or **5** (3.4 mmol, 1.0 equiv.), amine (20.4 mmol, 6.0 equiv.) and $NaCNBH_3$ (3.8 mmol, 250 mg, 1.1 equiv.) in anhydrous MeOH (10 mL) under Ar atmosphere. The resulting mixture was stirred at room temperature for 20 h. Upon completion, the reaction was quenched by adding conc. HCl to adjust pH to 1.0 and excess MeOH was removed under reduced pressure. The residue was then dissolved in water (20 mL), and the solution was washed with EtO_2 (3 × 10 mL). The pH of aqueous phases were then adjusted to 12.0 by using sat. NaOH solution, and the aqueous phases were extracted with EtO_2 (3 × 10 mL). To the combined organic phases were added water (10 mL) and *con.*HCl (keep pH below 1.0), the aqueous phase was collected which was then by addition of sat. NaOH solution to adjust the pH to 12.0. The aqueous solution was then repeatedly extracted with DCM. The combined organic phases were washed with brine (20 mL), dried over anhydrous $MgSO_4$ and concentrated *in vacuo* to give a pure racemic amine product standard **3a** and **5a**.

Protein Crystallisation

Screening of crystallization conditions was performed using commercially available INDEX (Hampton Research), PACT premier and CSSI/II (Molecular Dimensions) screens in 96-well sitting drop trays. Optimization was carried out in a 48-well sitting-drop format to obtain crystals for X-ray diffraction studies. For co-crystallization experiments, a 0.1 M stock solution of cofactor $NADP^+$ in water was prepared. Crystals of the IR91-$NADP^+$ complex were grown using IR91 concentrated to 15 mg mL^{-1} and complexed with 2 mM $NADP^+$. Crystals grew in conditions containing 0.1 M bis-tris-propane buffer at pH 5.5 containing 25% (w/v) PEG 3350 and 0.2 M Li_2SO_4. Crystals of IR91-$NADP^+$-**5** and IR91-**5a** were grown using IR91 at 11 mg mL^{-1} and complexed with 2 mM $NADP^+$ and 10 mM **5** or **5a** added from a concentrated stock solution in DMSO. Crystals grew in 0.1 M bis-tris-

propane buffer at pH 5.5 and 25% (w/v) PEG 3350 with 0.2 M $(NH_4)_2SO_4$. Crystals were harvested directly into liquid nitrogen with nylon CryoLoops™ (Hampton Research), using the mother liquor without any further cryoprotectant.

Data Collection, Structure Solution and Refinement

The datasets described in this report were collected at the Diamond Light Source, Didcot, Oxfordshire, U.K. on beamlines IO3 and I04-1. Data were processed and integrated using XDS[24] and scaled using SCALA[25] included in the Xia2[26] processing system. Data collection statistics are provided in **Table S1**. The crystal of IR91-$NADP^+$ and IR91-$NADP^+$-**5a** were obtained in space group $P2_1$, each with two molecules in the asymmetric unit; Crystals of IR91-$NADP^+$-**5** were obtained in space group $P2_12_12_1$, also with two molecules in the asu. The structure of IR91-$NADP^+$ was solved by molecular replacement using MOLREP[27] with the monomer of IRED 6JIT as the model. The structures were built and refined using iterative cycles in Coot[28] and REFMAC,[29] employing local NCS restraints in the refinement cycles. Following building and refinement of the protein and water molecules in each structure complex, residual density was observed in the omit maps at the dimer interfaces of each of the three structures, which could be clearly modelled as $NADP^+$. Additional omit density in the maps derived for IR91-$NADP^+$-**5** and IR91-$NADP^+$-**5a** could be modelled as 5-methoxy-2-tetralone and 5-methoxy-(*S*)-2-(*N*-methylamino)-tetralin respectively. The final structures of IR91-$NADP^+$, IR91-$NADP^+$-**5** and IR91- $NADP^+$-**5a** exhibited % R_{cryst}/R_{free} values of 23.3/25.3, 20.5/24.0 and 19.0/23.5 respectively. Refinement statistics for the structures are presented in **Table S1.** The structures of IR91-$NADP^+$, IR91-$NADP^+$-**5** and IR91-$NADP^+$-**5a** have been deposited in the Protein Databank (PDB) with accession codes **9R76**, **9R79** and **9R7A** respectively.

Biotransformations of **3** and **5** with IR91

To a flame dried round bottom flask containing a magnetic stirring bar was added the corresponding ketone **3** or **5** (0.1 mmol, 1.0 equiv.), $MeNH_2$.HCl (5.0 mmol, 337.5 mg, 50.0 equiv.), glucose (1.0 mmol, 180.2 mg, 10.0 equiv.), GDH (6 mg, 0.3 mg/mL), $NADP^+$ (0.01 mmol, 7.5 mg, 0.1 equiv.) and IR91 solution in Tris buffer (2 mL, 6 mg/mL) in Tris buffer (18 mL, pH 9). The resulting mixture was stirred at room temperature for 20 h. Upon completion, the reaction was adjusted to pH 12 by adding 2 M aq. NaOH. The solution was washed with DCM (3 × 15 mL). The combined organic phases were washed with brine (20 mL), dried over anhydrous $MgSO_4$ and concentrated *in vacuo* to give (*S*)-**3a** and (*S*)-**5a**. The conversion was determined by ^{1}H NMR in $CDCl_3$. The enantiomeric excess was measured by chiral HPLC. For **3a**: using an AD-H column, flow rate 1 mL/min, 99:1 hexane: IPA. For **5a**: using an IG column flow rate 1 mL/min, 97.5:2.5 hexane: IPA. Chromatography traces for racemic **3a** and the biotransformation product (*S*)-**3a** are shown in **Figure S11A** and **S11B**. Chromatography traces for racemic **5a** and the biotransformation product (*S*)-**5a** are shown in **Figure S11C** and **S11D**.

Mutagenesis of IR91

In order to investigate the contribution to catalysis of residue Y172 to the reactions catalysed by IR91, this residue was mutated to alanine (Y172A). The mutant was generated using InFusion® and established protocols[2] using the primers detailed in **Table S2**. Mutants W285A and E223A were purchased in pET-28a from Genscript. IR91 mutants were expressed and purified using the protocols described above for the wild-type IR91.

Supporting Information

Gene and amino acid sequences; PCR primers; SDS-PAGE gels; Kinetics; X-ray crystallography data; standard and chiral GC analysis conditions. NMR of products **3a** and **5a**.

Acknowledgements

We thank Mr Sam Hart and Dr Johan Turkenburg for X-ray data collection and the Diamond Light Source for access to beamlines I03 and I04-1 under grant MX24948. We also thank Dr David Entwhistle and colleagues at Codexis for the generous gift of glucose dehydrogenase GDH-105.

Keywords: Biocatalysis, Amine, Imine, NADPH, Imine Reductase

References

[1] G. Grogan and N. J. Turner, *Chem. Eur. J.*, **2016**, *22*, 1900-1907.
[2] J. Mangas-Sanchez, S. P. France, S. L. Montgomery, G. A. Aleku, H. Man, M. Sharma, J. I. Ramsden, G. Grogan and N. J. Turner, *Curr. Opin. Chem. Biol.*, **2017**, *37*, 19-25
[3] K. Mitsukura, M. Suzuki, K. Tada, T. Yoshida and T. Nagasawa, *Org. Biomol. Chem.*, **2010**, *8*, 4533-4535.
[4] F. Leipold, S. Hussain, D. Ghislieri and N. J. Turner, *ChemCatChem*, **2013**, *5*, 3410-3410
[5] S. Hussain, F. Leipold, H. Man, E. Wells, S. P. France, K. R. Mulholland, G. Grogan and N. J. Turner, *ChemCatChem*, **2015**, *7*, 579-583.
[6] N. Zumbrägel, P. Machui, J. Nonnhoff and H. Gröger, *J. Org. Chem.*, **2019**, *84*, 1440-1447.
[7] Y.-H. Zhang, F.-F. Chen, B.-B. Li, X.-Y. Zhou, Q. Chen, J.-H. Xu and G.-W. Zheng, *Org. Lett.*, **2020**, *22*, 3367-3372.
[8] A. K. Gilio, T. W. Thorpe, N. Turner and G. Grogan, *Chem. Sci.*, **2022**, *13*, 4697-4713.
[9] G. A. Aleku, S. P. France, H. Man, J. Mangas-Sanchez, S. L. Montgomery, M. Sharma, F. Leipold, S. Hussain, G. Grogan and N. J. Turner, *Nat. Chem.*, **2017**, *9*, 961-969.
[10] M. Schober, C. MacDermaid, A. A. Ollis, S. Chang, D. Khan, J. Hosford, J. Latham, L. A. F. Ihnken, M. J. B. Brown, D. Fuerst, M. J. Sanganee and G.-D. Roiban, *Nat. Catal.*, **2019**, *2*, 909-915.
[11] R. Kumar, M. J. Karmilowicz, D. Burke, M. P. Burns, L. A. Clark, C. G. Connor, E. Cordi, N. M. Do, K. M. Doyle, S. Hoagland, C. A. Lewis, D. Mangan, C. A. Martinez, E. L. McInturff, K. Meldrum, R. Pearson, J. Steflik, A. Rane and J. Weaver, *Nat. Catal.*, **2021**, *4*, 775-782.
[12] F.-F. Chen, X.-F. He, X.-X. Zhu, Z. Zhang, X.-Y. Shen, Q. Chen, J.-H. Xu, N. J. Turner and G.-W. Zheng, *J. Am. Chem. Soc.*, **2023**, *145*, 4015-4025.
[13] J. Steflik, A. Gilio, M. Burns, G. Grogan, R. Kumar, R. Lewis and C. Martinez, *ACS Catal.*, **2023**, *13*, 10065-10075.
[14] M. Rodríguez-Mata, A. Frank, E. Wells, F. Leipold, N. J. Turner, S. Hart, J. P. Turkenburg and G. Grogan, *ChemBioChem*, 2013, **14**, 1372-1379.
[15] T. Huber, L. Schneider, A. Präg, S. Gerhardt, O. Einsle and M. Müller, *ChemCatChem*, **2014**, *6*, 2248-2252.
[16] H. Man, E. Wells, S. Hussain, F. Leipold, S. Hart, J. P. Turkenburg, N. J. Turner and G. Grogan, *ChemBioChem*, **2015**, *16*, 1052-1059.
[17] S. P. France, R. M. Howard, J. Steflik, N. J. Weise, J. Mangas-Sanchez, S. L. Montgomery, R. Crook, R. Kumar and N. J. Turner, *ChemCatChem*, **2018**, *10*, 510-514.
[18] P. N. Scheller, S. Fademrecht, S. Hofelzer, J. Pleiss, F. Leipold, N. J. Turner, B. M. Nestl and B. Hauer, *ChemBioChem*, **2014**, *15*, 2201-2204.
[19] M. Sharma, J. Mangas-Sanchez, S. P. France, G. A. Aleku, S. L. Montgomery, J. I. Ramsden, N. J. Turner and G. Grogan, *ACS Catal.*, **2018**, *8*, 11534-11541
[20] Q. Chen, B.-B. Li, L. Zhang, X.-R. Chen, X.-X. Zhu, F.-F. Chen, M. Shi, C.-C. Chen, Y. Yang, R.-T. Guo, W. Liu, J.-H. Xu and G.-W. Zheng, *ACS Catal.*, **2022**, *12*, 14795-14803.
[21] J. Citoler, V. Harawa, J. R. Marshall, H. Bevinakatti, J. D. Finnigan, S. J. Charnock and N. J. Turner, *Angew. Chem. Int. Ed.*, **2021**, *60*, 24456-24460.

[22] L. Holm, A. Laiho, P. Törönen and M. Salgado, *Protein Sci.*, **2023**, *32*, e4519.
[23] J. G. Cannon, J. A. Perez, J. P. Pease, J. P. Long, J. R. Flynn, D. B. Rusterholz and S. E. Dryer, *J. Med. Chem.*, 1980, **23**, 745−749.
[24] W. Kabsch, *Acta Crystallogr. Sect. D*, 2010, **66**, 125-132.
[25] P. Evans, *Acta Crystallogr. Sect. D D*, 2006, **62**, 72-82.
[26] G. Winter, *J. Appl. Crystallogr.*, 2010, **43**, 186-190.
[27] A. Vagin and A. Teplyakov, *J. Appl. Crystallogr.*, 1997, **30**, 1022-1025.
[28] P. Emsley and K. Cowtan, *Acta Crystallogr. Sect. D*, 2004, **60**, 2126-2132.
[29] G. N. Murshudov, A. A. Vagin and E. J. Dodson, *Acta Crystallogr. Sect. D*, 1997, **53**, 240-255.

Entry for the Table of Contents

COMMUNICATION

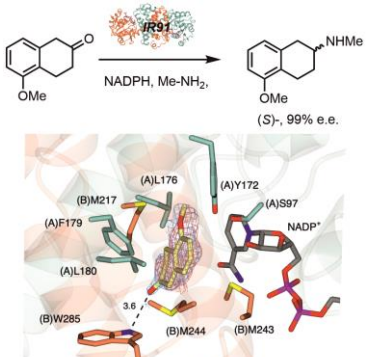

The structure of the (*S*)-selective 'Tyrosine' Imine Reductase (IRED) IR91 from *Kribbella flavida* is presented in complex with its ketone substrate and (*S*)-amine product, revealing for the first time the interactions of substrate and product with an IRED of this type acting in a reductive aminase mode.

*Krishnan Srinivas, Amelia K. Gilio, Mahima Sharma, Lawrence Green, Alexander Ascham, Jack Domenech, Balázs Pogrányi, Jiacheng Li, Scott P. France, Russell D. Lewis, William P. Unsworth and Gideon Grogan**

*Page No. – **Page No.***

Structures of 'Tyrosine-IRED' IR91 from *Kribbella flavida* in Complex with a Reductive Amination Substrate and Product